Clinical Cancer Research

SIRT1/PGC1α-Dependent Increase in Oxidative Phosphorylation Supports Chemotherapy Resistance of Colon Cancer

Thomas T. Vellinga[1], Tijana Borovski[1], Vincent C.J. de Boer[2], Szabolcs Fatrai[1], Susanne van Schelven[1], Kari Trumpi[1], Andre Verheem[1], Nikol Snoeren[1], Benjamin L. Emmink[1], Jan Koster[3], Inne H.M. Borel Rinkes[1], and Onno Kranenburg[1]

Abstract

Purpose: Chemotherapy treatment of metastatic colon cancer ultimately fails due to development of drug resistance. Identification of chemotherapy-induced changes in tumor biology may provide insight into drug resistance mechanisms.

Experimental Design: We studied gene expression differences between groups of liver metastases that were exposed to preoperative chemotherapy or not. Multiple patient-derived colonosphere cultures were used to assess how chemotherapy alters energy metabolism by measuring mitochondrial biomass, oxygen consumption, and lactate production. Genetically manipulated colonosphere-initiated tumors were used to assess how altered energy metabolism affects chemotherapy efficacy.

Results: Gene ontology and pathway enrichment analysis revealed significant upregulation of genes involved in oxidative phosphorylation (OXPHOS) and mitochondrial biogenesis in metastases that were exposed to chemotherapy. This suggested chemotherapy induces a shift in tumor metabolism from glycolysis towards OXPHOS. Indeed, chemotreatment of patient-derived colonosphere cultures resulted in an increase of mitochondrial biomass, increased expression of respiratory chain enzymes, and higher rates of oxygen consumption. This was mediated by the histone deacetylase sirtuin-1 (SIRT1) and its substrate, the transcriptional coactivator PGC1α. Knockdown of SIRT1 or PGC1α prevented chemotherapy-induced OXPHOS and significantly sensitized patient-derived colonospheres as well as tumor xenografts to chemotherapy.

Conclusions: Chemotherapy of colorectal tumors induces a SIRT1/PGC1α-dependent increase in OXPHOS that promotes tumor survival during treatment. This phenomenon is also observed in chemotherapy-exposed resected liver metastases, strongly suggesting that chemotherapy induces long-lasting changes in tumor metabolism that potentially interfere with drug efficacy. In conclusion, we propose a novel mechanism of chemotherapy resistance that may be clinically relevant and therapeutically exploitable. *Clin Cancer Res; 21(12); 2870–9. ©2015 AACR.*

Introduction

Colon cancer is one of the most common and deadliest types of cancer. Mortality is mainly the consequence of metastatic growth in secondary organs like liver and lungs. Chemotherapeutic drugs that have proven to be effective in the treatment of metastatic colon cancer are 5-fluorouracil (5-FU), oxaliplatin, and irinotecan, which together prolong median survival from approximately 6 months to approximately 2 years (1). However, most tumors are either intrinsically resistant to these drugs or acquire resistance during treatment. Consequently, disease progression following systemic therapy occurs in the vast majority of cases (1).

To rationally develop therapeutic approaches that can overcome drug resistance, it is essential to understand the underlying mechanisms. "Omics" technologies are nowadays increasingly used to determine the (epi-)genetic underpinnings of drug resistance (2, 3). In colon cancer, this has resulted in the identification of gene signatures that can identify intrinsically drug-resistant tumor subtypes (4–7). In the current study, we use such technologies to study how drug resistance develops in colon cancer patients that have been treated with chemotherapy.

Normal, healthy cells mainly use OXPHOS for energy production. Cancer cells, however, face an impressive metabolic challenge due to rapid cell growth and frequent divisions, which forces them to adjust their energy metabolism to meet these demands (8). In addition to the (in-)activation of specific oncogenes and/or tumor suppressor genes, the bioenergetic status of tumor cells is influenced by microenvironmental factors such as availability of oxygen (hypoxia) and nutrients (9–11). These factors also induce changes in the metabolic state of the cells, allowing them to survive the harsh tumor environment. All this results in a predominant shift in metabolism of tumor cells from OXPHOS towards aerobic glycolysis

[1]Department of Surgery, University Medical Center Utrecht, Utrecht, the Netherlands. [2]Department of Clinical Chemistry, Laboratory Genetic Metabolic Diseases, Academic Medical Center, University of Amsterdam, Amsterdam, the Netherlands. [3]Department of Oncogenomics, Academic Medical Center, University of Amsterdam, Amsterdam, the Netherlands.

Note: Supplementary data for this article are available at Clinical Cancer Research Online (http://clincancerres.aacrjournals.org/).

Corresponding Author: Onno Kranenburg, Department of Surgery, University Medical Center Utrecht, Heidelberglaan 100, Utrecht 3584CX, the Netherlands. Phone: 318-8755-8632; Fax: 313-0254-1944; E-mail: o.kranenburg@umcutrecht.nl

doi: 10.1158/1078-0432.CCR-14-2290

Translational Relevance

Many metastasized colorectal tumors are intrinsically resistant to chemotherapy, while others acquire drug resistance during treatment. With the current therapeutic modalities, disease progression is virtually inevitable. The design of therapeutic strategies that target drug resistance needs to be based on a thorough understanding of its mechanistic principles. In the current study, we used transcriptomics data of chemotherapy-exposed and chemo-naïve liver metastases to identify a novel pathway of drug resistance, involving an increased dependency on mitochondrial biogenesis and oxidative phosphorylation. We have subsequently used colonosphere cultures to demonstrate a causal relationship between chemotherapy treatment and altered energy metabolism and have identified SIRT1 and PGC1α as key factors in the process. Suppression of these factors increases the efficacy of chemotherapy *in vitro* and in mice bearing colonosphere-initiated human tumor xenografts. We propose that therapeutic targeting of oxidative energy metabolism should be explored as a strategy to prevent acquired drug resistance.

(Warburg effect; ref. 12). Although in various tumors, glycolysis prevails as the main, and in some cases even exclusive source of ATP, it is important to note that intense glycolysis is not mandatory for all tumor types and some cancers do rely on OXPHOS for ATP production (13, 14). Tumor metabolism has received increased attention over the last decade, mainly in relation to proliferation and specific metabolic alterations. Only recently the metabolic state has been implicated in tumor drug resistance (15, 16). Targeting tumor metabolism is now actively being studied as an alternative approach to overcome this problem. Drugs that limit the uptake of nutrients or interfere with their use in anabolic pathways have shown efficacy as resistance-modulating agents in several preclinical models (17–20). However, the link between tumor metabolism and drug resistance is highly complex, it depends on multiple parameters such as oxygen and nutrient availability or the specific drugs that are being used, and the underlying mechanisms still remain to be elucidated (15). In the current study, we used transcriptomics data of liver metastases from chemotherapy-treated and chemo-naïve colon cancer patients to identify a novel pathway of drug resistance, involving a change in energy metabolism. We show that upon chemotherapy, cancer cells shift their metabolism from glycolysis towards OXPHOS. This process is regulated via SIRT1–PGC1α signaling pathway and, as a consequence, increases the resistance of cells to chemotherapy.

Materials and Methods

Cell culture

Human colorectal tumor specimens were obtained from patients undergoing colon or liver resection for primary or metastatic adenocarcinoma, respectively, in accordance with the local ethical committee on human experimentation (protocol #09-145). Informed consent was obtained from all patients. Human colonosphere cultures were isolated and propagated as described (21).

Flow cytometry

A total of 300 nmol/L Mitotracker Green (Invitrogen) was added to the cultures for 30 minutes. Cells were resuspended in PBS containing 0.5 μg/mL propidium iodide to exclude dead cells and analyzed with FACSCalibur (BD Biosciences). Experiments were performed in triplicates, and the results are depicted as an average of at least three independent experiments. Data are presented as mean ± SD.

Antibodies and reagents

Western blot analysis: anti-SIRT1 (Millipore), anti-cleaved caspase-3, and anti-cleaved PARP (Cell Signaling Technology), MitoProfile Total OXPHOS Rodent WB antibody cocktail (Abcam), anti-β-actin (Novus Biologicals). Immunhistochemistry: COXIV (Abcam). SIRT1 inhibitors: nicotinamide (Sigma), EX527 (Sigma), Tenovin-6 (Cayman Chemical).

Lentiviral transduction

shSIRT1 plasmids were obtained from Sigma (TRCN-0000018979) and (TRCN0000018983). shSCR plasmid (SHC002) was used as a control. shPGC1α construct was a kind gift from Prof. P. Puigserver from the Dana-Farber Cancer Institute (Boston, MA). Lentiviral particles were generated by transfecting 293T cells with pLKO and packaging vectors using Fugene (Roche). Transduced cells were selected with puromycin.

Rescue experiment

CRC29 cells were transfected with expression vectors encoding shSIRT1 (TRCN0000018983) and FLAG-SIRT1 either alone or combined using standard manufacturer Lipofectamine3000 (Life Technologies) protocol. Forty-eight hours following transfection, cells were treated with chemotherapy for 24 hours and mitochondrial content was analyzed using Mitotracker as described previously.

Immunohistochemistry

COXIV staining was performed on formalin-fixed paraffin-embedded sections from colorectal liver metastasis. Samples were deparaffinized and rehydrated. Citrate buffer (pH 6.0) was used for antigen retrieval. Primary antibody: anti-COXIV (Abcam).

Quantitative real-time PCR

Total RNA from colonosphere cultures or tissue samples was isolated using manufacturer's protocol (RNeasy Mini Kit). cDNA was synthesized using iScriptcDNA Synthesis Kit (Bio-Rad Laboratories). The amplification was performed in an iCyclerthermocycler (Bio-Rad Laboratories) using iQ SYBR Green Supermix (Bio-Rad Laboratories). mRNA expression levels were quantified using iCycler software (Bio-Rad Laboratories) and were normalized to RPL13a. The primers used for RT-qPCR are listed in Supplementary Table S1. All samples were analyzed in triplicates.

Animal experiments

Colonospheres were dissociated into single-cell suspension with Accumax and 5×10^4 cells expressing shSCR or shSIRT1 were mixed with Matrigel (BD Biosciences) at 1:1 ratio and injected subcutaneously into the flanks of 12-week-old male CBy.Cg-Foxn1nu/J mice. Tumor growth was measured weekly and tumor volumes were calculated ($V = a \times b^2 \times 0.5263$), "a" being the maximal width and "b" maximal orthogonal width. Six

weeks after the injection, we started the chemotreatment. Chemotherapy was administered weekly intraperitoneally, oxaliplatin (10 mg/kg) and 5-FU (100 mg/kg). Control mice received PBS only. When tumors reached a volume of 1,500 mm^3 mice were sacrificed. For tumor analysis, outliers (±>3 times SD from the mean) were excluded. For analysis of necrosis, the slides were digitized and analyzed via Aperio Imagescope (Leica Biosystems). The surface of necrotic areas (excluding the necrotic centre) were measured and calculated as a percentage of the total area (excluding the necrotic centre). All experiments were performed in accordance with University of Utrecht institutional animal welfare guidelines.

Cell death analysis

Colonospheres were plated in 96-well plate and either treated or not with oxaliplatin (10 μg/mL) plus 5-FU (10 μg/mL) for 48 hours. Before the measurement, total cell population was labeled with DRAQ5 (Abcam) and live cells were labeled with Calcein Green AM (Life Technologies). Fluorescence was measured using the Arrayscan (Thermo Scientific).The percentage of dead cells was calculated by normalizing the levels of intensity to and expressed as a relative percentage of the plate-averaged vehicle-treated control. Experiments were performed in triplicates and the results display the average of at least three independent experiments. Data are presented as mean ± SD.

Bioinformatics analyses

We used our previously generated dataset containing gene expression profiles of 119 liver metastases (22) deposited at Array Access under accession number: E-TABM-1112. The dataset was uploaded into the R2 microarray analysis and visualization platform and analyzed. Differential gene expression between tumor groups was performed with the "Find differential expression between groups" option (single gene ANOVA, $P < 0.05$), and selecting each available clinical variable separately. To find differentially represented pathways in chemotherapy-treated versus nontreated tumors the resulting gene list was analyzed for enrichment of Gene Ontology terms in chemotherapy-treated versus naïve tumor subgroups with the Gene Set Analysis option. In addition, differentially represented pathways were analyzed with the "KEGG pathway finder" (Minimal t test, $P < 0.0001$).

OCR and ECAR measurement

The Seahorse XF96 Extracellular Flux Analyzer (Seahorse Biosciences) was used to obtain real-time measurements of oxygen consumption rate (OCR) and extracellular acidification rates (ECAR) in cells. Colonospheres treated with or without chemotherapy were dissociated into single cells using Accumax. Cells were reconstituted in culture medium and seeded in 96-well Seahorse culture plates at a density of 40,000 cells/well. For analysis of ECAR, cells were reconstituted in Seahorse medium. Cells were allowed to settle for 1 hour before measurements. OCR and ECAR were analyzed using 2′ mix followed by 3′ measurement cycle. Oligomycin (Sigma) was injected at a final concentration of 2 μmol/L, carbonyl cyanide 4-(trifluoromethoxy)phenylhydrazone (FCCP, Sigma) at 3 μmol/L, antimycin A (Sigma) at 5 μmol/L and rotenone (Sigma) at 2 μmol/L. Basal OCR is the mean OCR from 0′, 5′, 10′, 15′ and maximal OCR is the mean OCR from 37′, 42′, 47′. For ECAR measurements 2-deoxyglucose (Sigma) was injected at a final concentration of 100 mmol/L. OCR and ECAR were normalized to protein or DNA content determined by BCA assay or Cyquant assay (Invitrogen). Data are presented as mean ± SEM.

Statistical analysis

All values are presented as mean ± SEM or SD. The Student t test (unpaired, two-tailed) or one-way ANOVA was performed to analyze whether differences between the groups are statistically significant. Differences with a P value of less than 0.05 were considered statistically significant.

Results

Chemotherapy of colorectal liver metastases induces lasting changes in gene expression

The majority of patients with metastatic colorectal cancer receive chemotherapy, either alone or in combination with surgery. To identify mechanisms that could underlie chemotherapy resistance we used gene expression profiles of 119 liver metastases, of which 64 had received neoadjuvant chemotherapy (i.e., before resection; ref. 22). Of all clinical variables tested, neoadjuvant chemotherapy was by far most strongly associated with changes in gene expression (Supplementary Table S2). Variables that were not correlated with significant changes in gene expression included various clinical scoring systems, tumor recurrence, tumor size, and location, CEA levels, extent of resection, and disease-free and overall survival (Supplementary Table S2). We identified 481 genes whose expression was significantly ($P < 0.05$) downregulated and 613 genes whose expression was significantly upregulated in chemotherapy-exposed tumors (Fig. 1A and Supplementary Table S3). Interestingly, as the mean interval time between the last cycle of chemotherapy and resection of the metastases was 17 weeks (5–35), the observed differences in gene expression are persistent and long-lasting.

Genes regulating mitochondrial biogenesis and OXPHOS are upregulated in chemotherapy-exposed liver metastases

To identify the biologic pathways that are represented by the differentially expressed genes between chemotherapy-exposed and chemotherapy-naïve tumors, we performed gene ontology analysis. This showed that the "mitochondrial respiration chain" (GO0005746) was most significantly different between the two tumor groups ($P = 2.2e{-}5$). In addition, the "KEGG pathway finder" identified OXPHOS as the most significantly upregulated pathway in chemotherapy-treated tumors ($P = 4.1e{-}4$; Supplementary Table S4). Similar results were obtained with Ingenuity Pathway Analysis (Supplementary Table S4). The 14 differentially expressed OXPHOS pathway genes were all upregulated in chemo-treated tumors. The electron transport chain consists of 5 distinct enzyme complexes. Chemo-treated metastases expressed high levels of multiple components of complexes I, III, IV, and V (Supplementary Table S5 and Fig. 1B). In addition, we found that mitochondrial biogenesis genes, in particular mitochondrial ribosomal proteins, like Mrpl11, Mrps16 and Mrps12, were also expressed to significantly higher levels in chemotherapy-treated tumors when compared with nontreated tumors (Supplementary Table S5 and Fig. 1B).

Next, we sought to validate the above results by performing immunohistochemistry analysis of the expression of COXIV, a component of mitochondrial complex IV and a frequently used marker for mitochondrial content, in pathologic tissue sections.

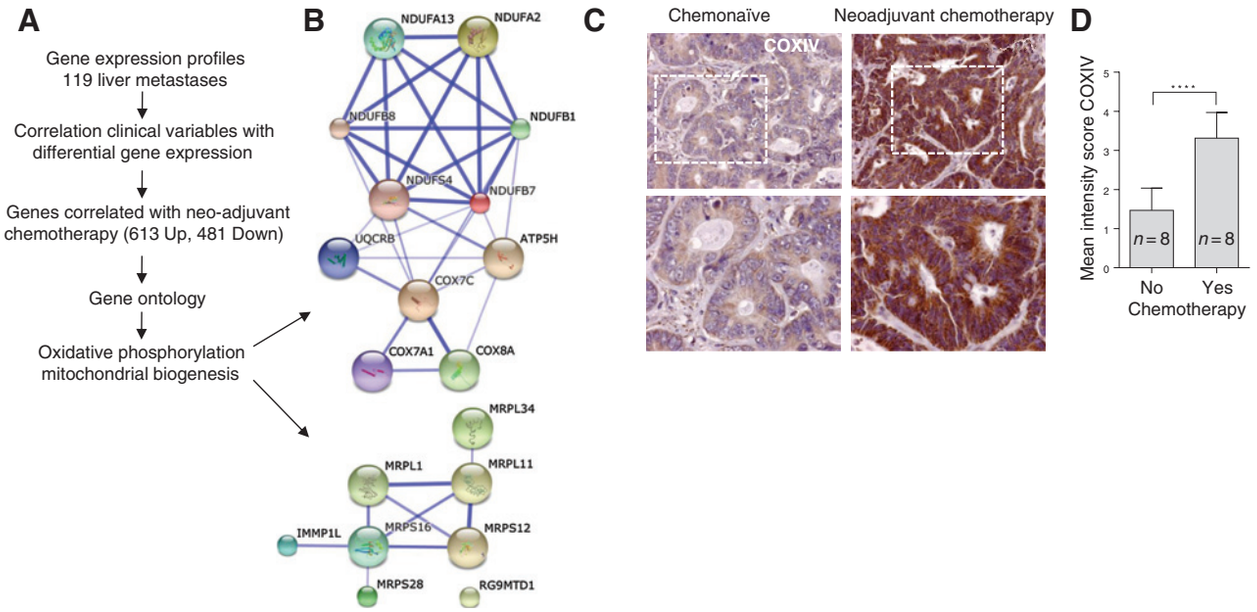

Figure 1.

Chemotherapy of colon cancer liver metastases is associated with increased expression of genes involved in mitochondrial biogenesis and OXPHOS. A, overview of the study design. B, analysis of the interaction between genes that were significantly upregulated in chemotherapy-treated tumors by using the Search Tool for the Retrieval of Interacting Genes/Proteins. The clusters reflecting OXPHOS and mitochondrial biogenesis are shown. C, cytochrome *c* oxidase (COXIV) immunohistochemistry on paraffin-embedded tissue sections of liver metastasis either treated or not with chemotherapy. D, quantification of the COXIV staining intensity ($n = 8$ per group). Significance was determined with the Student *t* test. ****, $P < 0.0001$.

For this, we used an independent series of colorectal liver metastases that had either received neoadjuvant chemotherapy ($n = 8$) or not ($n = 8$). Indeed, we identified a markedly higher intensity of COXIV staining in sections from liver metastases that were treated with neoadjuvant chemotherapy as compared to chemo-naïve tumors (Fig. 1C and Supplementary Fig. S1). Double-blind scoring of the stained sections confirmed that COXIV staining was significantly higher in treated compared with nontreated metastases (Fig. 1D). These findings establish that electron transport chain pathway is significantly upregulated in chemotherapy-treated liver metastases from two independent patient cohorts both at the mRNA and protein level.

Chemotherapy treatment induces oxidative energy metabolism in patient-derived colonospheres

Upregulation of mitochondrial biogenesis and electron transport chain pathways suggested that chemotherapy may alter energy metabolism in colorectal tumors by shifting cellular metabolism towards mitochondrial OXPHOS. To test this experimentally, we made use of a panel of colonosphere cultures established from primary colorectal tumors (CRC09, CRC16, and CRC29) and liver metastases (L145 and L167; ref. 21). First, we assessed how exposure of colonospheres to oxaliplatin and 5-FU, the first-line cytotoxic treatment for metastatic colorectal cancer, alters mitochondrial mass in these cells. Control and drug-exposed colonospheres were stained with the fluorescent Mitotracker probe and mitochondrial content was determined by FACS analysis. Chemotherapy significantly increased mitochondrial mass in five distinct colonosphere cultures, irrespective of whether they were derived from primary tumors ($n = 3$) or liver metastases ($n = 2$; Fig. 2A). Furthermore, similar to the upregulation of COXIV staining in chemotherapy-treated tumors *in vivo*, protein levels of complex IV as well as complex I, II, and III were strongly upregulated following chemotherapy exposure (Fig. 2B), demonstrating that the colonosphere cultures reflect the changes observed *in vivo*.

Chemotherapy-induced increase in mitochondrial content and expression of OXPHOS enzymes suggested that chemotherapy-exposed tumor cells may shift from a glycolytic to a more oxidative energy metabolism. To test this directly, we determined OCR and ECAR of colonosphere cells by Seahorse analysis. Both basal and maximum OCRs were significantly increased in chemotherapy-treated colonopheres in three independent cultures (Fig. 2C). In parallel, ECAR was significantly reduced. 2-Deoxyglucose injection normalized the ECAR levels of both chemo-treated and nontreated cells to baseline levels. Both maximal and basal ECAR were reduced, demonstrating that the overall glycolytic capacity of the cells was reduced (Fig. 2C). Combined, lowered ECAR and enhanced OCR show that chemotherapy-treated colonospheres rely more on mitochondrial OXPHOS than nontreated ones. To further explore the effect of chemotherapy on glycolysis, we analyzed the expression of glycolytic enzymes, respiratory chain components, and SIRT1 following chemotherapy exposure of two independent colonosphere lines (L145; CRC09) by qRT-PCR analysis. We found that chemotherapy reduced the expression of the glycolytic enzymes PKM2, PFKP, and hexokinase 2, while the respiratory chain components NDUFS3 and ATP5G1 as well as SIRT1 showed increased expression (Supplementary Fig. S2). It should be noted, however, that a correlation between mRNA and protein levels is not always found (23, 24). ATP synthesis rates through glycolysis and OXPHOS, respectively, were calculated (refs. 25, 26; Supplementary Table S6). Glycolysis was the predominant source of ATP production in two independent nontreated colonosphere lines (L145, CRC09).

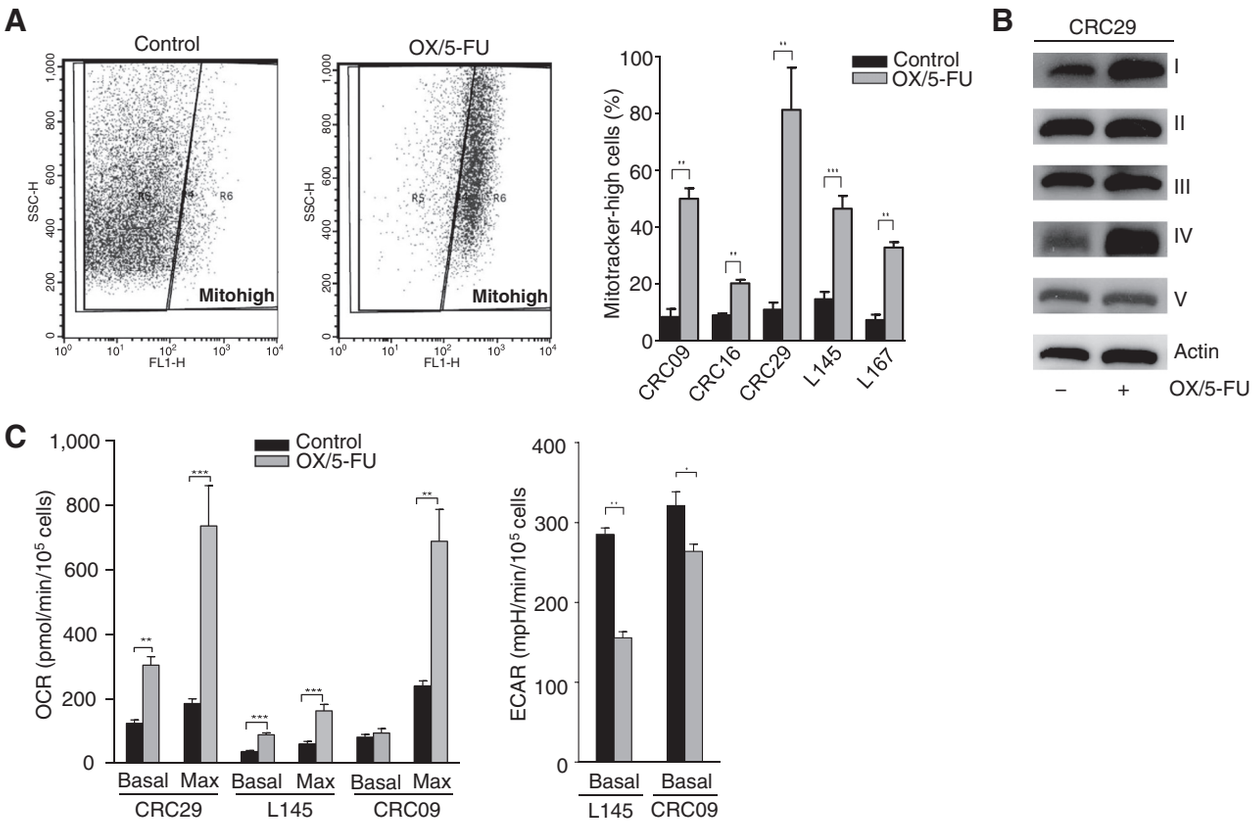

Figure 2.

Chemotherapy increases OXPHOS in colonosphere cultures. A, colonosphere cultures derived from five distinct tumors were exposed to chemotherapy [oxaliplatin 10 μg/mL + 5-FU 10 μg/mL] for 72 hours. Mitotracker Green was used to determine chemotherapy-induced changes in mitochondrial content. FACS dot plots show an increase in mitotracker signal in colonosheres upon chemotherapy. Quantification of the FACS data is shown on the right. B, colonosphere cultures were treated as in A for 48 hours. Western blot analysis demonstrates an increase in OXPHOS complexes after chemotherapy. C, colonosphere cultures were treated as in A for 48 hours. The basal and maximal OCRs and basal ECARs were measured on the Seahorse Bioanalyzer. Significance was determined with the Student *t* test. *, $P < 0.05$; **, $P < 0.01$; ***, $P < 0.001$.

Assessment of the generality of this phenomenon would require analysis of glycolysis- and OXPHOS-dependent ATP production rates in a large series of colonosphere lines. However, while chemotherapy treatment reduced glycolytic ATP synthesis, it increased ATP synthesis through OXPHOS (Supplementary Table S6).

Chemotherapy induces SIRT1 to promote oxidative energy metabolism

To identify potential regulators of the observed chemotherapy-induced metabolic changes, we reanalyzed the gene list that was upregulated in chemotherapy-treated tumors and searched for factors that could regulate mitochondrial biogenesis and/or OXPHOS. SIRT1 encodes sirtuin-1, a NAD^+-dependent histone deacetylase that is activated in response to DNA damage and plays a key role in mitochondrial biogenesis (27, 28). SIRT1 was also in the top 5% of most significantly upregulated genes following chemotherapy (Fig. 3A; Supplementary Table S3). For these reasons, we hypothesized that SIRT1 could play a causative role in altering cellular energy metabolism following chemotherapy. None of the other Sirtuins (SIRT2-7) were expressed to higher levels in chemotherapy-treated tumors. Treatment of colonosphere cultures with oxaliplatin and 5-FU also greatly enhanced SIRT1 protein levels, thus demonstrating a causal relationship between chemotherapy and increased SIRT1 expression (Fig. 3B). The SIRT3 enzyme regulates mitochondrial respiration by directly deacetylating respiratory enzymes and could thereby control changes in energy homeostasis following chemotherapy exposure. However, neither SIRT3 mRNA nor protein levels were changed in tumors or colonospheres exposed to chemotherapy (Fig. 3A and B). Next, we analyzed whether inhibition of SIRT1 would interfere with the increase in mitochondrial mass triggered by chemotherapy. To this end, we used the sirtuin inhibitors nicotinamide (NAM), EX-527, and Tenovin-6 (TV-6). All three compounds impaired the chemotherapy-induced enhancement of mitochondrial mass (Fig. 3C). Importantly, NAM also completely prevented the chemotherapy-induced increase in basal and maximum OCR (Fig. 3D and Supplementary Fig. S3).

Next, we analyzed whether suppression of SIRT1 expression by RNA interference would have an impact on the chemotherapy-induced increase in mitochondrial mass. We suppressed SIRT1 in CRC29 and L145 colonospheres by expressing two independent shRNAs and used scrambled (SCR) hairpins as controls (Fig. 4A). Consistent with the SIRT1 inhibitor data, we found that SIRT1

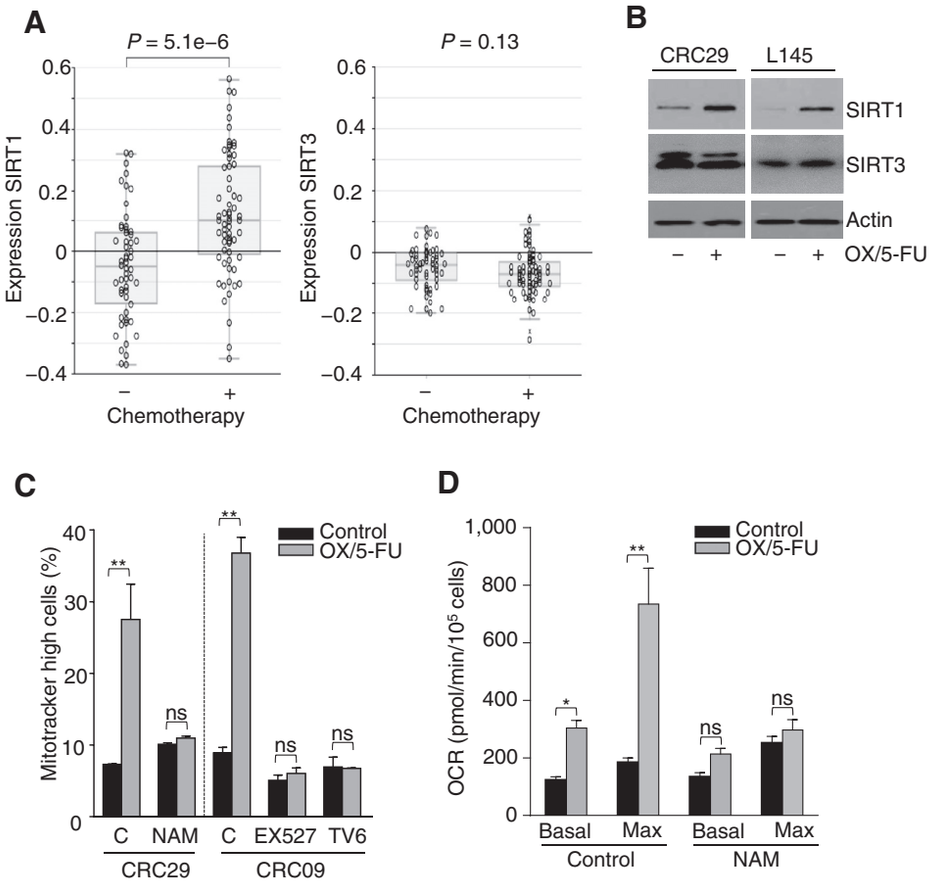

Figure 3.
SIRT1 inhibition prevents chemotherapy-induced OXPHOS. A, the gene expression profiles of 119 liver metastases (22) were used to analyze SIRT1 and SIRT3 expression in liver metastases that had been exposed to chemotherapy ($n = 64$) or not ($n = 55$). The P value was determined by ANOVA. B, colonosphere cultures were treated with oxaliplatin (10 μg/mL) plus 55-FU (10 μg/mL) for 24 hours. Western blot analysis shows an increase in SIRT1 protein levels upon the treatment. SIRT3 protein levels did not alter upon chemotherapy. C, colonosphere cultures were treated as in B for 48 hours, with or without SIRT1 inhibitors nicotinamide (NAM; 30 mmol/L), EX527 (30 μmol/L), or TV6 (10 μmol/L). Mitochondrial content was assessed as in Fig. 2A. D, CRC29 were treated with chemotherapy and NAM as in B for 48 hours. The basal and maximal OCRs are from the same experiment as depicted in Fig. 2C. The basal and maximal OCRs were determined on the Seahorse Bioanalyzer. Significance was determined with the Student t test. *, $P < 0.05$; **, $P < 0.01$.

knockdown (KD) prevented the chemotherapy-induced elevation in mitochondrial mass (Fig. 4A). Furthermore, expression of complex I–IV was upregulated by drug treatment, but was not induced in SIRT1 KD cells (Fig. 4B). Because NAM suppressed the increase in OCR upon drug-treatment, we performed similar Seahorse experiments in cells with KD of SIRT1. Eliminating SIRT1 expression did not impact OCR in nontreated cells, whereas in chemotherapy-treated cells OCR was greatly reduced (Fig. 4C), again demonstrating that SIRT1 is required for the induction of mitochondrial OXPHOS by chemotherapy. To control for nonspecific off-target RNAi effects, we performed a rescue experiment using the SIRT1-targeting shRNA#2 (which targets a noncoding region in the SIRT1 mRNA) and an expression vector encoding FLAG-tagged SIRT1 that is not targeted by shRNA#2. Forty-eight hours after transfection, colonosphere cultures were treated with oxaliplatin (10 μg/mL) and 5-FU (10 μg/mL) for 24 hours and mitochondrial content was analyzed. Consistent with the previous results, SIRT1 KD blocked the chemotherapy-induced increase in mitochondrial biomass. Coexpression of FLAG-SIRT1 completely restored the chemotherapy-induced increase in mitochondrial biomass, demonstrating that the effect of the knockdown vector was indeed due to SIRT1 suppression (Fig. 4D).

SIRT1 controls mitochondrial biogenesis by deacetylating and activating PGC1α, which is a master regulator of mitochondrial function (29). PGC1α has been shown to be essential for directing the transcriptional program for enhancing mitochondrial biogenesis and function (30). To test whether mitochondrial biogenesis in chemotherapy-treated colonospheres is indeed activated via the SIRT1/PGC1α-axis, we expressed shRNAs directed against PGC1α in CRC29 colonospheres, which resulted in efficient suppression of PGC1α protein expression (Fig. 5A). Again, chemotherapy caused an increase in mitochondrial mass and stimulated expression of OXPHOS enzymes in control cells, but not in colonospheres in which PGC1α was suppressed (Fig. 5B and C). Together, these findings demonstrate that SIRT1 and PGC1α are necessary for triggering mitochondrial biogenesis in response to chemotherapy in patient-derived colonosphere cultures.

SIRT1 and PGC1α protect colon cancer cells against chemotherapy

In addition to mitochondrial biogenesis, SIRT1 is involved in multiple DNA repair processes and both SIRT1 and PGC1α play a role in the defense against reactive oxygen species (ROS) generated in high amounts by chemotherapy (31). Furthermore, chemotherapy-induced DNA damage greatly increases the ATP demand (32). Therefore, we studied whether suppression of SIRT1 or PGC1α would affect the sensitivity of cancer cells to chemotherapy. Strikingly, already after 16 hours of chemotherapy treatment of PGC1α KD cells, cleaved PARP and cleaved caspase-3 were detected, whereas in control cells only after 48 hours low levels of cleaved products became apparent (Fig. 6A). Also in

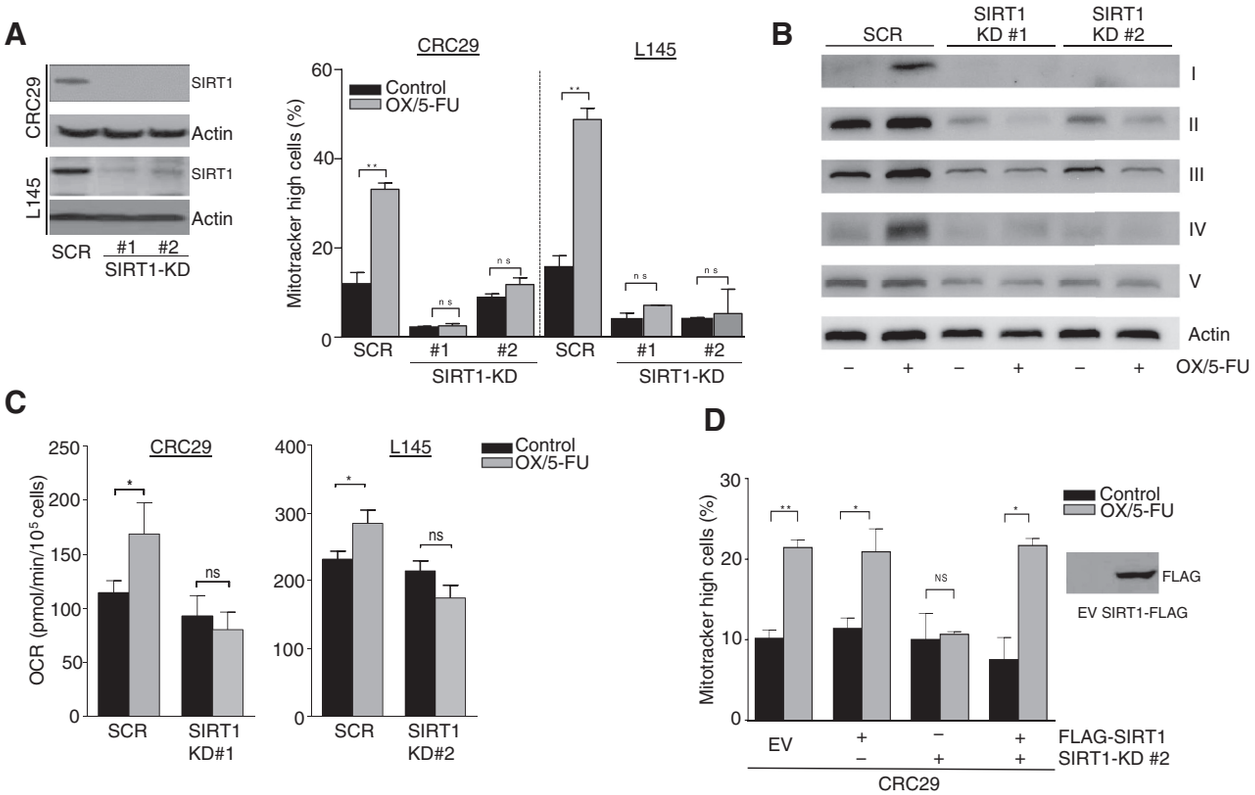

Figure 4.
SIRT1 KD prevents chemotherapy-induced OXPHOS. A, colonosphere cultures were transduced with lentiviral vectors expressing two independent shRNAs targeting SIRT1 or a control vector expressing a scrambled shRNA (SCR). SIRT1 protein levels were determined by Western blot analysis. SIRT1 KD and SCR were treated with oxaliplatin (10 μg/mL) plus 5-FU (10 μg/mL) for 48 hours and mitochondrial content was analyzed as in Fig. 2A. B, SIRT1 KD and SCR were treated as in A. Expression levels of OXPHOS complexes were measured by Western blot analysis. C, SIRT1 KD and SCR were treated with chemotherapy as in A. The basal OCRs were measured on the Seahorse Bioanalyzer. L145-scr shows an increased basal OCR when compared with parental cells (Fig. 2C), possibly/most likely due to the transduction and/or selection process. D, colonospheres were transfected with expression vectors encoding shSIRT1 and FLAG-SIRT1 either alone or in combination as indicated. Forty-eight hours after transfection, cultures were treated with oxaliplatin (10 μg/mL) plus 5-FU (10 μg/mL) for 24 hours and mitochondrial content was analyzed as in Fig. 2A. Significance was determined with the Student *t* test. *, $P < 0.05$; **, $P < 0.01$.

SIRT1 KD cells, drug treatment resulted in markedly increased levels of both cleaved PARP and cleaved caspase-3 as compared with treated control cells (Fig. 6A). Increased levels of cleaved PARP and cleaved caspase-3 indicate that SIRT1/PGC1α KD cells might commit to a cell death program faster than control cells. Therefore, we analyzed chemotherapy-induced cell death using

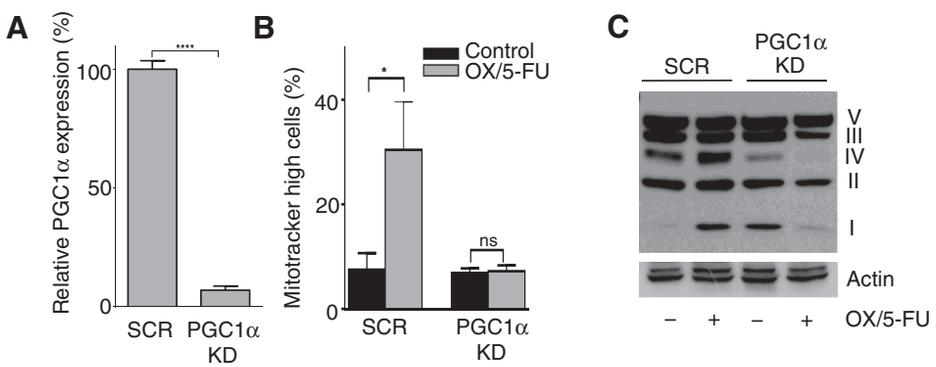

Figure 5.
PGC1α KD prevents chemotherapy-induced OXPHOS. A, CRC29 were transduced with lentiviral vector expressing shPGC1α or shSCR. PGC1α mRNA levels were determined by qRT-PCR. B, PGC1α KD and SCR were treated with oxaliplatin (10 μg/mL) plus 5-FU (10 μg/mL) for 48 hours and mitochondrial content was analyzed as in Fig. 2A. C, PGC1α KD and SCR were treated as in B. Protein levels of OXPHOS enzymes were measured by Western blot analysis. Significance was determined with the Student *t* test. *, $P < 0.05$; ***, $P < 0.001$.

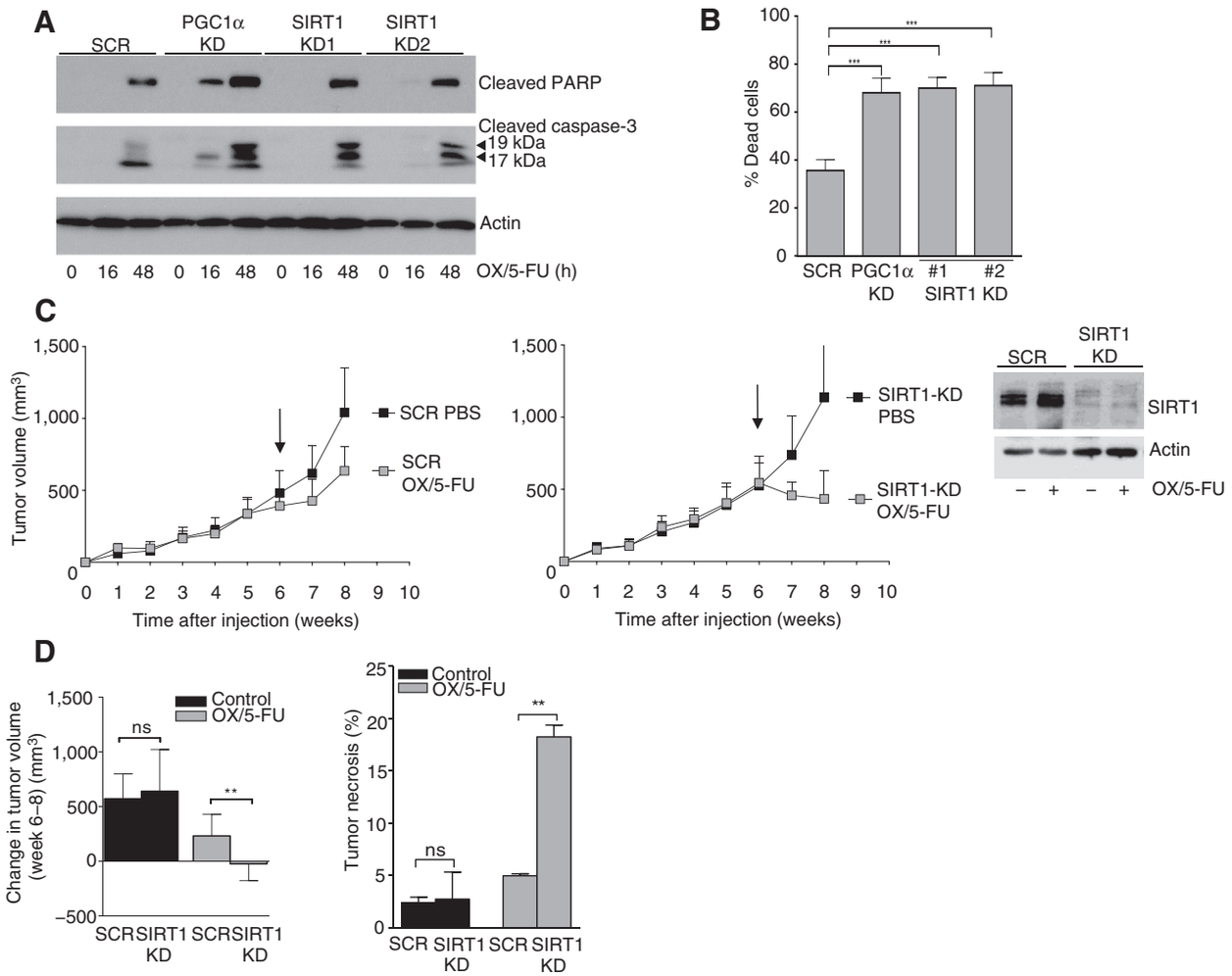

Figure 6.

SIRT1 and PGC1α protect colon cancer cells against chemotherapy. A, SIRT1 KD, PGC1α KD and SCR were treated with chemotherapy for 16 and 48 hours. Cleaved PARP and cleaved caspase-3 levels were determined by Western blot analysis. Arrowheads indicate the cleaved forms of caspase-3. B, SIRT1 KD, PGC1α KD, and SCR were treated with chemotherapy for 48 hours and percentage of dead cells was measured by cytotoxicity assay, as described in Materials and Methods. C, SIRT1 KD and SCR were injected subcutaneously into nude mice. From 6 weeks on, mice were treated with oxaliplatin plus 5-FU or PBS as described in Materials and Methods. The experiment was terminated when the tumors reached 1,500 mm^3 volume. The tumor growth curves are plotted as mean ± SEM ($n = 9$ per group). Arrows, start of treatment. SIRT1 protein levels in SIRT1 KD and SCR xenograft tumors were determined by WB. D, absolute change in tumor volume from start treatment (week 6) until stop treatment (week 8). Quantification of the necrotic areas in tumor tissue sections from SIRT1 KD and SCR tumors as described in Materials and Methods. Significance was determined with the Student t test. **, $P < 0.01$; ***, $P < 0.001$.

Arrayscan analysis. Exposure of control cells to chemotherapy for 48 hours resulted in approximately 35% cell death. Strikingly, in both PGC1α and SIRT1 KD cells, the percentage of cell death was approximately 2-fold higher (Fig. 6B), demonstrating that PGC1α and SIRT1 make the colonospheres more resistant to chemotherapy.

Finally, to evaluate the impact of SIRT1 KD on tumor growth and chemosensitivity *in vivo*, control, and SIRT1 KD colonospheres were subcutaneously injected in nude mice. Mice were treated with oxaliplatin in combination with 5-FU 6 weeks after injection of cells. As shown in Fig. 6C, SIRT1 KD tumors had a marked regression in response to oxaliplatin/5-FU treatment. In contrast, chemotherapy did not induce regression of control tumors. Overall effect of chemotherapy at the end of the experiment was significantly more pronounced in SIRT1 KD compared with control tumors (Fig. 6D). Western blot analysis showed that SIRT1 KD was maintained in the tumors throughout the experiment (Fig. 6C). Histochemical analysis of tumor tissue sections further showed that chemotherapy induced significantly more tumor necrosis in SIRT1 KD tumors when compared with control tumors (Fig. 6D). Collectively, these results demonstrate that chemotherapy induces a shift in tumor energy metabolism from glycolysis to OXPHOS via SIRT1/PGC1α and that this protects tumor cells from cytotoxic damage.

Discussion

Preventing disease progression by overcoming drug resistance is a major goal in medical oncology. In the current study, we have identified OXPHOS and the SIRT1/PGC1α pathway as an

important contributor to therapy resistance and a potential therapeutic target.

Cells may rapidly adapt their metabolic pathways in response to changes in the microenvironment, including the availability of growth factors, nutrients, and oxygen (33). Our data indicate that genotoxic stress also alters energy metabolism. We show that in response to chemotherapy colonospheres engage a SIRT1/PGC1α-dependent (partial) reversion of the Warburg effect, shifting glycolysis to OXPHOS, and that this supports survival after treatment. This is in line with previous reports correlating increased mitochondrial oxidative energy metabolism to chemoresistance of tumor cells. Metabolic characterization of glioma cells revealed an enhanced oxidative metabolism in drug-resistant cells when compared with drug-sensitive cells (34). Importantly, we show that tumors of chemotherapy-treated cancer patients show lasting gene expression changes that reflect activation of the OXPHOS program. This strongly suggests that chemotherapy-induced gene expression alterations could potentially underlie tumor resistance in a long run, making our data clinically relevant.

Why would cancer cells shift their metabolism in favor of OXPHOS? Under normal conditions, the amount of ATP produced through aerobic glycolysis is sufficient to support tumor cell growth and basal DNA repair activity. However, cellular ATP demand is greatly increased following chemotherapy as many enzymes involved in DNA repair, drug efflux, and drug detoxification require ATP (35, 36). As OXPHOS is the most efficient way to generate ATP, it is not surprising that cancer cells would increase this pathway at times of high ATP demand. The role of SIRT1 in cancer is still controversial as evidence for both tumor-promoting and -suppressing activities have been found and the impact of SIRT1 on cell viability seem to be highly context-dependent (37). In the current report, we show that all tumor-derived colonosphere cultures and xenografts in which SIRT1 (or PGC1α) was suppressed, were sensitized to drug treatment. This is in line with previously published data showing that SIRT1 KD sensitized Saos2 osteosarcoma cells to doxorubicin although this study did not identify increased OXPHOS as the critical downstream SIRT1 effector pathway (38). Likewise, high expression of PGC1α in melanoma cells causes an increase in oxidative energy metabolism, increased expression of ROS-detoxifying enzymes, and resistance to ROS-inducing drugs (39). Upon PGC1α inhibition, such OXPHOS-dependent melanoma cells reverted to a glycolytic energy metabolism (40).

Mechanistically, chemotherapy-induced DNA damage results in increased expression of SIRT1, possibly via the multifunctional DNA repair protein and transcriptional coactivator APE1 (41). SIRT1-mediated deacetylation reactions consume and require NAD^+ as a substrate (42). NAD^+ levels rise when cells experience an energy deficit, for instance during fasting or exercise, and presumably also after chemotherapy-induced DNA damage (43). Indeed, SIRT1 is recruited to sites of DNA damage and participates in several DNA repair processes (27, 44). In addition, SIRT1 deacetylates PGC1α, leading to its activation as a transcriptional coactivator (45). PGC1α acts in concert with several transcription factors to stimulate the expression of genes involved in mitochondrial biogenesis and respiration, resulting in increased OXPHOS (46, 47).

Taken together, our study provides insight into how colorectal tumors shift their energy metabolism when challenged with chemotherapy. We demonstrate that chemotherapy induces OXPHOS in colon cancer cells via the SIRT1/PGC1α axis to help them survive treatment. Further investigations aimed at targeting this program in combination with chemotherapy deserve further attention and may ultimately increase response rates in the treatment of colon cancer.

Disclosure of Potential Conflicts of Interest

No potential conflicts of interest were disclosed.

Authors' Contributions

Conception and design: T.T. Vellinga, O. Kranenburg

Development of methodology: T.T. Vellinga, T. Borovski, V.C.J. de Boer, S. Fatrai

Acquisition of data (provided animals, acquired and managed patients, provided facilities, etc.): T.T. Vellinga, V.C.J. de Boer, S. van Schelven, A. Verheem, N. Snoeren, B.L. Emmink

Analysis and interpretation of data (e.g., statistical analysis, biostatistics, computational analysis): T.T. Vellinga, T. Borovski, V.C.J. de Boer, S. van Schelven, K. Trumpi, A. Verheem, J. Koster, I.H.M. Borel Rinkes, O. Kranenburg

Writing, review, and/or revision of the manuscript: T.T. Vellinga, T. Borovski, V.C.J. de Boer, K. Trumpi, I.H.M. Borel Rinkes, O. Kranenburg

Administrative, technical, or material support (i.e., reporting or organizing data, constructing databases): T.T. Vellinga, S. van Schelven, K. Trumpi

Study supervision: T. Borovski, I.H.M. Borel Rinkes, O. Kranenburg

Grant Support

This work was supported by grants from the Dutch Cancer Society (KWF; UU2011-5226 to T.T. Vellinga; UU2011-5135 to T. Borovski and S. van Schelven; and UU2009-4367 to B.L. Emmink) and Foundation Friends of the University Medical Center Utrecht (to K. Trumpi).

The costs of publication of this article were defrayed in part by the payment of page charges. This article must therefore be hereby marked *advertisement* in accordance with 18 U.S.C. Section 1734 solely to indicate this fact.

Received September 3, 2014; revised February 11, 2015; accepted February 27, 2015; published OnlineFirst March 16, 2015.

References

1. Lucas AS, O'Neil BH, Goldberg RM. A decade of advances in cytotoxic chemotherapy for metastatic colorectal cancer. Clin Colorectal Cancer 2011;10:238–44.
2. Longley DB, Allen WL, Johnston PG. Drug resistance, predictive markers and pharmacogenomics in colorectal cancer. Biochim Biophys Acta 2006;1766:184–96.
3. Crea F, Danesi R, Farrar WL. Cancer stem cell epigenetics and chemoresistance. Epigenomics 2009;1:63–79.
4. Melo DSE, Wang X, Jansen M, Fessler E, Trinh A, de Rooij LP, et al. Poor-prognosis colon cancer is defined by a molecularly distinct subtype and develops from serrated precursor lesions. Nat Med 2013; 19:614–8.
5. Roepman P, Schlicker A, Tabernero J, Majewski I, Tian S, Moreno V, et al. Colorectal cancer intrinsic subtypes predict chemotherapy benefit, deficient mismatch repair and epithelial-to-mesenchymal transition. Int J Cancer 2014;134:552–62.
6. Sadanandam A, Lyssiotis CA, Homicsko K, Collisson EA, Gibb WJ, Wullschleger S, et al. A colorectal cancer classification system that associates cellular phenotype and responses to therapy. Nat Med 2013; 19:619–25.

7. Schlicker A, Beran G, Chresta CM, McWalter G, Pritchard A, Weston S, et al. Subtypes of primary colorectal tumors correlate with response to targeted treatment in colorectal cell lines. BMC Med Genomics 2012; 5:66.
8. Vander Heiden MG, Cantley LC, Thompson CB. Understanding the Warburg effect: the metabolic requirements of cell proliferation. Science 2009;324:1029–33.
9. Semenza GL, Roth PH, Fang HM, Wang GL. Transcriptional regulation of genes encoding glycolytic enzymes by hypoxia-inducible factor 1. J Biol Chem 1994;269:23757–63.
10. Semenza GL. HIF-1 mediates metabolic responses to intratumoral hypoxia and oncogenic mutations. J Clin Invest 2013;123:3664–71.
11. Obre E, Rossignol R. Emerging concepts in bioenergetics and cancer research: Metabolic flexibility, coupling, symbiosis, switch, oxidative tumors, metabolic remodeling, signaling and bioenergetic therapy. Int J Biochem Cell Biol 2015;59C:167–81.
12. Warburg O. On the origin of cancer cells. Science 1956;123:309–14.
13. Jose C, Bellance N, Rossignol R. Choosing between glycolysis and oxidative phosphorylation: a tumor's dilemma? Biochim Biophys Acta 2011;1807: 552–61
14. Moreno-Sánchez R, Rodríguez-Enríquez S, Marín-Hernández A, Saavedra E. Energy metabolism in tumor cells. FEBS J 2007;274:1393–418.
15. Butler EB, Zhao Y, Munoz-Pinedo C, Lu J, Tan M. Stalling the engine of resistance: targeting cancer metabolism to overcome therapeutic resistance. Cancer Res 2013;73:2709–17.
16. Zhao Y, Butler EB, Tan M. Targeting cellular metabolism to improve cancer therapeutics. Cell Death Dis 2013;4:e532.
17. Cao X, Fang L, Gibbs S, Huang Y, Dai Z, Wen P, et al. Glucose uptake inhibitor sensitizes cancer cells to daunorubicin and overcomes drug resistance in hypoxia. Cancer Chemother Pharmacol 2007;59: 495–505.
18. Cufi S, Corominas-Faja B, Vazquez-Martin A, Oliveras-Ferraros C, Dorca J, Bosch-Barrera J, et al. Metformin-induced preferential killing of breast cancer initiating CD44+CD24−/low cells is sufficient to overcome primary resistance to trastuzumab in HER2+ human breast cancer xenografts. Oncotarget 2012;3:395–8.
19. Maschek G, Savaraj N, Priebe W, Braunschweiger P, Hamilton K, Tidmarsh GF, et al. 2-deoxy-D-glucose increases the efficacy of adriamycin and paclitaxel in human osteosarcoma and non-small cell lung cancers *in vivo*. Cancer Res 2004;64:31–4.
20. Lu CW, Lin SC, Chien CW, Lin SC, Lee CT, Lin BW, et al. Overexpression of pyruvate dehydrogenase kinase 3 increases drug resistance and early recurrence in colon cancer. Am J Pathol 2011;179:1405–14.
21. Emmink BL, van Houdt WJ, Vries RG, Hoogwater FJ, Govaert KM, Verheem A, et al. Differentiated human colorectal cancer cells protect tumor-initiating cells from irinotecan. Gastroenterology 2011;141: 269–78.
22. Snoeren N, van Hooff SR, Adam R, van Hillegersberg R, Voest EE, Guettier C, et al. Exploring gene expression signatures for predicting disease free survival after resection of colorectal cancer liver metastases. PLoS ONE 2012;7:e49442.
23. Maier T, Güell M, Serrano L. Correlation of mRNA and protein in complex biological samples. FEBS Lett 2009;583:3966–73.
24. Tian Q, Stepaniants SB, Mao M, Weng L, Feetham MC, Doyle MJ, et al. Integrated genomic and proteomic analyses of gene expression in Mammalian cells. Mol Cell Proteomics 2004;3:960–9.
25. Davis EJ, Davis-van Thienen WI. An assessment of the role of proton leaks in the mechanistic stoichiometry of oxidative phosphorylation. Arch Biochem Biophys 1991;289:184–6.
26. Birket MJ, Orr AL, Gerencser AA, Madden DT, Vitelli C, Swistowski A, et al. A reduction in ATP demand and mitochondrial activity with neural differentiation of human embryonic stem cells. J Cell Sci 2011;124:348–58.
27. Wang RH, Sengupta K, Li C, Kim HS, Cao L, Xiao C, et al. Impaired DNA damage response, genome instability, and tumorigenesis in SIRT1 mutant mice. Cancer Cell 2008;14:312–23.
28. Knight JR, Milner J. SIRT1, metabolism and cancer. Curr Opin Oncol 2012;24:68–75.
29. Lagouge M, Argmann C, Gerhart-Hines Z, Meziane H, Lerin C, Daussin F, et al. Resveratrol improves mitochondrial function and protects against metabolic disease by activating SIRT1 and PGC-1alpha. Cell 2006;15: 1109–22.
30. Puigserver P. Tissue-specific regulation of metabolic pathways through the transcriptional coactivator PGC1-alpha. Int. J Obes 2005;29:S5–9.
31. Weijl NI, Cleton FJ, Osanto S. Free radicals and antioxidants in chemotherapy-induced toxicity. Cancer Treat Rev 1997;23:209–40.
32. Zhou Y, Tozzi F, Chen J, Fan F, Xia L, Wang J , et al. Intracellular ATP levels are a pivotal determinant of chemoresistance in colon cancer cells. Cancer Res 2012;72:304–14.
33. Shlomi T, Benyamini T, Gottlieb E, Sharan R, Ruppin E. Genome-scale metabolic modeling elucidates the role of proliferative adaptation in causing the Warburg effect. PLoS Comput Biol 2011;7:e1002018.
34. Oliva CR, Moellering DR, Gillespie GY, Griguer CE. Acquisition of chemoresistance in gliomas is associated with increased mitochondrial coupling and decreased ROS production. PLoS ONE 2011;6:e24665.
35. Gottesman MM, Fojo T, Bates SE. Multidrug resistance in cancer: role of ATP-dependent transporters. Nat Rev Cancer 2002;2:48–58.
36. Osley MA, Tsukuda T, Nickoloff JA. ATP-dependent chromatin remodeling factors and DNA damage repair. Mutat Res 2007;618:65–80.
37. Deng CX. SIRT1, is it a tumor promoter or tumor suppressor? Int J Bio Sci 2009;5:147–52.
38. Chu F, Chou PM, Zheng X, Mirkin BL, Rebbaa A. Control of multidrug resistance gene mdr1 and cancer resistance to chemotherapy by the longevity gene sirt1. Cancer Res 2005;65:10183–7.
39. Vazquez F, Lim JH, Chim H, Bhalla K, Girnun G, Pierce K, et al. PGC1alpha expression defines a subset of human melanoma tumors with increased mitochondrial capacity and resistance to oxidative stress. Cancer Cell 2013;23:287–301.
40. Lim JH, Luo C, Vazquez F, Puigserver P. Targeting mitochondrial oxidative metabolism in melanoma causes metabolic compensation through glucose and glutamine utilization. Cancer Res 2014;74:3535–45.
41. Antoniali G, Lirussi L, D'Ambrosio C, Dal Piaz F, Vascotto C, Casarano E, et al. SIRT1 gene expression upon genotoxic damage is regulated by APE1 through nCaRE-promoter elements. Mol Biol Cell 2014;25:532–47.
42. Canto C, Auwerx J. Targeting sirtuin 1 to improve metabolism: all you need is NAD(+)? Pharmacol Rev 2012;64:166–87.
43. Canto C, Auwerx J. Caloric restriction, SIRT1 and longevity. Trends Endocrinol Metab 2009;20:325–31.
44. Martin SG, Laroche T, Suka N, Grunstein M, Gasser SM. Relocalization of telomeric Ku and SIR proteins in response to DNA strand breaks in yeast. Cell 1999;97:621–33.
45. Gerhart-Hines Z, Rodgers JT, Bare O, Lerin C, Kim SH, Mostoslavsky R, et al. Metabolic control of muscle mitochondrial function and fatty acid oxidation through SIRT1/PGC-1alpha. EMBO J 2007;26:1913–23.
46. Zhong L, Mostoslavsky R. Fine tuning our cellular factories: sirtuins in mitochondrial biology. Cell Metab 2011;13:621–6.
47. Scarpulla RC. Metabolic control of mitochondrial biogenesis through the PGC-1 family regulatory network. Biochim Biophys Acta 2011;1813: 1269–78.